Square-Planar Complexes

DOI: 10.1002/anie.201106091

High-Spin Square-Planar Co^{II} and Fe^{II} Complexes and Reasons for Their Electronic Structure**

*Stefanie A. Cantalupo, Stephanie R. Fiedler, Matthew P. Shores, Arnold L. Rheingold, and Linda H. Doerrer**

More than half a century of intense investigation in coordination compounds has laid a firm foundation for our understanding of the ligand fields in transition-metal complexes.[1] Complexes of the heavier 4d and 5d metals are generally low spin, whereas the spin of 3d metal complexes can be high or low, depending on ligand characteristics. The number and type of donor atoms, ligand substituents, and the presence or absence of chelate rings all influence metal spin states. A combination of data-mining and detailed computational study have quantified recently these empirical observations.[2,3] In spite of such variety, there are still some types of metal complexes that are rarely observed.

The stereospinomers[3] of high-spin, square-planar complexes, for example, are extremely rare because the large separation of the $d_{x^2-y^2}$ orbital from the rest of the d-manifold favors low-spin electron configurations for d^n with $n > 4$, and four-coordinate compounds are rare for d^4 systems which could have all four low-lying d orbitals half filled. Known d^4 examples include multiple Cr^{II} species,[4] a Mn^{III} species,[5] and one[6] Nb^{I} complex. The rarity of this geometry and spin-state combination is demonstrated by only a handful of examples with late 3d metals. An interesting $\{NiO_2N_2\}$ d^8 system[7] is known whose high-spin examples are subtly dependent on ligand substitution. Until the structure was confirmed[8] as tetrameric with octahedral coordination at the Co center, $[Co(acac)_2]$ was postulated to have square-planar geometry based on magnetic and spectroscopic data that differed from tetrahedral complexes.[9] A search of the Cambridge Structural Database (V 5.32)[10] for Fe and Co complexes in a four-coordinate environment with τ_4 parameter[11] < 0.25 and magnetic susceptibility data revealed five high-spin d^6 Fe^{II} complexes with macrocyclic or chelating N_4[12,13] and O_4[14,15] coordination, and three high-spin d^7 Co^{II} complexes[12,16,17] with varied ligand systems. A complete description of the CSD search and results can be found in the Supporting Information. Herein we report a unique pair of high-spin, square-planar $\{MO_4\}$ species.

Our group has prepared several families of homoleptic fluorinated aryloxide and alkoxide complexes of 3d metals. We have extensively investigated the high-spin aryloxide compounds $[M(OAr)_4]^{2-}$, M = Fe,[18] Co,[19] Ni,[20] and Cu[19,21] and $[M(OAr)_5]^{2-}$, M = Fe,[18] in which OAr = OC_6F_5 or 3,5-$OC_6H_3(CF_3)_2$, as well as the high-spin alkoxide compounds $[M(OC_4F_9)_3]^{1-}$, M[22] = Fe, Co, Cu and $[M(OC_4F_9)_4]^{2-}$, M = Co,[22] Ni.[20] Spectroscopic[20] and computational[18] work have shown that these fluorinated ligands are medium field ligands, on par with OH^- and F^-, and stronger than NCO^-. The electron-withdrawing power of extensively fluorinated ligands reduces the π-donor character of the O atom, such that bridging is not observed and mononuclear species are readily prepared.

More recently, we have begun studies of the chelating perfluoropinacolate ligand, $ddfp^{2-}$.[23] Magnetic susceptibility and elemental analysis data were reported for $K_2[M(ddfp)_2]$, (M = Mn, Ni, Cu) for which square-planar geometry was proposed.[24] An octahedral bis-H_2O adduct, $(Me_4N)_2[Co(OH_2)_2(ddfp)_2]$ has been proposed based on elemental analysis data.[25]

Despite the relative ease in making the $[M(ddfp)_2]^{2-}$ complexes with first-row transition metals, no examples of M = Co^{II} or Fe^{II} have been published. We now report a high-spin, square-planar Co^{II} complex, $\{K(DME)_2\}_2[Co(ddfp)_2]$ (**1**), and the analogous high-spin, square-planar Fe^{II} complex $\{K(DME)_2\}_2[Fe(ddfp)_2]$ (**2**). We also provide a discussion of three other square-planar $\{MO_4\}$ species from the recent literature whose composition and spin-state characteristics clarify the ligand requirements for the highly unusual high-spin, square-planar combination in late row 3d metals.

Compound **1** has been prepared as pale pink crystals as shown in Equation (1), and is stable in an inert atmosphere and in various organic solvents, but yields a brown oil upon prolonged exposure to air. Iron-containing **2**, and the Zn^{II} derivative, $\{K(DME)_2\}_2[Zn(ddfp)_2]$ (**3**), were similarly prepared as purple-pink, and colorless crystals, respectively. No

$$M(Base)_2 + 2\,H_2ddfp \xrightarrow[2)\ 2\ KN(SiMe_3)_2,\ DME,\ 12\ h,\ N_2,\ RT]{1)\ toluene,\ 12\ h,\ N_2,\ RT} \{K(DME)_2\}_2[M(ddfp)_2] \quad M = Co(1), Fe(2), Zn(3) \qquad (1)$$

[*] S. A. Cantalupo, Prof. Dr. L. H. Doerrer
Department of Chemistry, Boston University
590 Commonwealth Avenue, Boston, MA 02215 (USA)
E-mail: doerrer@bu.edu
S. R. Fiedler, Prof. Dr. M. P. Shores
Department of Chemistry, Colorado State University
Fort Collins, CO 80523-1872 (USA)
Prof. Dr. A. L. Rheingold
Department of Chemistry and Biochemistry, University of California San Diego
9500 Gilman Drive, La Jolla, CA 92093-0358 (USA)

[**] This work was supported by Boston University, NSF (CHE 0910647 and CHE 0619339 for the purchase of an NMR spectrometer), Department of Energy (DE-SC0007055), ACS Petroleum Research Fund 48022-AC3, and NSF CRIF 0840418 for the purchase of an EPR spectrometer. We would also like to thank Colorado State University and NSF (CHE-1058889) for financial support.

Supporting information for this article is available on the WWW under http://dx.doi.org/10.1002/anie.201106091.

reaction of **1** or **2** with the Lewis bases THF or Et_3N was observed. Details are provided in the Supporting Information.

All compounds crystallized with two molecules of DME coordinated to each K^+ cation, $\{K(DME)_2\}_2[M(ddfp)_2]$. Tables of X-ray data collection parameters, selected distances, and angles can be found in the Supporting Information in Tables S1 and S2. The structure of **1** is shown in Figure 1, in which the rigorous $\{CoO_4\}$ planarity is clear. The Co atom is at the center of inversion and lies within the best $\{O_4\}$ plane. The average Co–O bond length is 1.9513(12) Å. The K^+ ions in **1** interact with the O atoms on the ligand at an average distance of 2.6784(13) Å. The average O-Co-O chelate angle is 84.30(4)°. The O atoms bridged by the K^+ ion form an O-Co-O angle of 95.70(4)°. The *trans* O-Co-O angle is perfectly linear, leading to a τ_4 value of 0, clearly indicating square-planar geometry. The structure of **2** is shown in Figure S1 and is isostructural to **1**, again with $\tau_4 = 0$. The average Fe–O bond length is 1.9692(12) Å and the K^+ interactions with the O atoms on the anion are at a distance of 2.690(1) Å. The O-Fe-O chelate angle 83.34(5)° and the angle bridged by the K^+ ion is 96.66(5)°. The closest intermolecular contact to the transition-metal ion (not shown) is 5.2682(1) Å from Co to H(14A) in **1** and 5.2877(2) Å from Fe to H(14B) in **2**, clearly demonstrating the four-coordinate nature of these species.

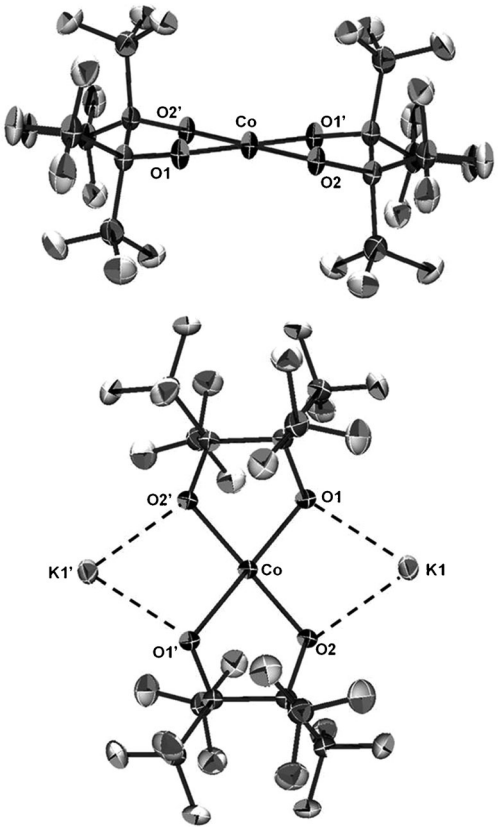

Figure 1. Top: ORTEP diagram of the anion of **1**. Bottom: ORTEP diagram of **1** showing K···O interactions. Solvent molecules removed for clarity. Ellipsoids are set at 50% probability. Selected bond lengths [Å] and angles [°]: Co–O1 1.9516(12), Co–O2 1.9510(12); O1-Co-O2 95.70(4), O1-Co-O2′ 84.30(4), O1-Co-O1′ 180.[48]

Details about the structure of **3** are in the Supporting Information. The average Zn–O distance at 1.944(3) Å is slightly shorter than the Co–O distance in compound **1**, and there are two K···O interactions at an average distance of 2.756(4) Å and one K···F interaction at 3.052(8) Å. The O-Zn-O angle bridged by the K^+ ion is 108.71(14)° and the angle subtended by the $ddfp^{2-}$ ligand is 87.4(2)°, resulting in $\tau_4 = 0.64$. The Zn^{II} derivative does not exhibit a perfect tetrahedral geometry because of the bridging $\{K(DME)\}^+$ ions and constraints of the five-membered chelate ring.

The UV/Vis spectra of **1**, 335 ($\varepsilon = 16$), 375 (31), 390 (33), and 525 nm ($21\,M^{-1}cm^{-1}$), and **2**, 395 ($\varepsilon = 15$) and 553 nm ($11\,M^{-1}cm^{-1}$), have small extinction coefficients owing to the Laporte-forbidden nature of the transitions. The electronic spectra are clearly distinct from both the well-known tetrahedral and octahedral species. The tetrahedral $[CoCl_4]^{2-}$ has two features at around 650 ($\varepsilon = 550$) and 675 nm ($590\,M^{-1}cm^{-1}$) with a smaller feature at 600 nm ($360\,M^{-1}cm^{-1}$),[28] and the analogous high-spin $[FeCl_4]^{2-}$ has features in the near-infrared region at 2470 nm ($80\,M^{-1}cm^{-1}$).[29] The octahedral $[M(H_2O)_6]^{2+}$ complexes have distinct absorbances at 560 nm ($5\,M^{-1}cm^{-1}$) for Co^{II} [28] and two features at 1205 nm and 961 nm with extinction coefficients of about $1\,M^{-1}cm^{-1}$ for Fe^{II}.[29]

The solution magnetic moment for **1** was determined by the Evans method[30] to be 4.89 μ_B (2.99 emu K mol^{-1}), larger than the spin-only value for $S = {}^3/_2$ of 3.87 μ_B. The magnetic moments for $[CoCl_4]^{2-}$ (4.59 μ_B) and $\{Co(acac)_2\}_4$ (4.93 μ_B per Co) also have significant unquenched orbital contributions, but more in the latter. The solution magnetic moment of **2** in $[D_8]$THF was determined to be 5.52 μ_B (3.81 emu K mol^{-1}), larger than the spin-only value for $S = 2$ of 4.89 μ_B. Both Co^{II} and Fe^{II} compounds are commonly observed to have orbital contributions to their magnetic susceptibilities.[31]

The temperature-dependent $\chi_M T$ data for zero-field cooled crystalline **1** are presented in Figure 2. The room temperature value of 2.91 emu K mol^{-1} is larger than expected

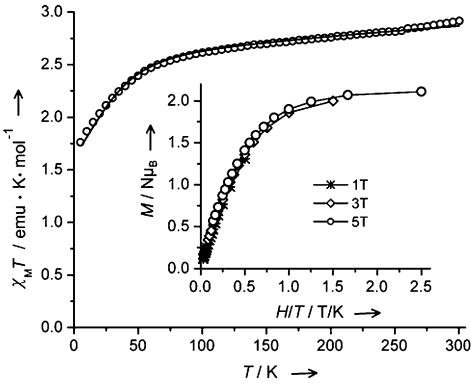

Figure 2. Temperature dependence of $\chi_M T$ for **1**, measured at 0.1 T. The best fit to the data obtained from MagSaki[26] is shown as a solid line. Inset: reduced field dependence of the magnetization for **1** at three selected fields. Lines shown are guides for the eye. Data collected at six fields (0.1–5 T) and lines of best fit obtained from ANISOFIT[27] are shown in Figure S4.

(1.875 emu K mol^{-1}) for the spin-only contributions of an $S = {}^3/_2$ complex with $g = 2.00$, but common for Co^{II}. These values are also consistent with those observed for the reported {CoN$_4$}[12,17,32] and {CoN$_2$P$_2$}[16] examples of square-planar high-spin Co^{II}. The $\chi_M T$ value decreases gradually from 2.91 to 2.54 emu K mol^{-1} at 75 K, followed by a more rapid decrease to 1.76 emu K mol^{-1} at 5 K. Even at low temperature, the susceptibility values are not consistent with a low-spin $S = {}^1/_2$ ground state (expected 0.375 emu K mol^{-1}). Others have reported similar room temperature $\chi_M T$ values for tetrahedral $S = {}^3/_2$ complexes, but $\chi_M T \ll 1$ emu K mol^{-1} for $S = {}^1/_2$ complexes.[33] The decrease below 75 K is likely due to zero-field splitting and not a spin-state change. The small kink in the $\chi_M T$ values at approximately 260 K does not occur for powdered samples encased in eicosane (Figure S3). Low-temperature magnetization data show near superposition of isofield lines (Figure 2, inset and S4), and saturate at 2.1 N μ_B. Since an unreasonably large average g value (> 3.00) would be required to support an $S = {}^1/_2$ assignment, the magnetization saturation value is more consistent with assignment of an $S = {}^3/_2$ ground state.

Although orbital effects in Co^{II} complexes complicate the determination of spin state from susceptibility data alone,[34] the data shown in Figure 2 are consistent with the maintenance of $S = {}^3/_2$ throughout the measured temperature range. The MagSaki[26] program was employed to fit the data for **1** to a high-spin, axially distorted, Co^{II} octahedral model, using the Hamiltonian [Eq. (2)]:[35]

$$H = -({}^3/_2)\kappa\lambda \mathbf{L}\,\mathbf{S} + \beta[(-{}^3/_2)\kappa \mathbf{L} + g_e\,\mathbf{S}] \qquad (2)$$

The program uses three parameters to fit the susceptibility data for mononuclear complexes: a spin-orbit coupling parameter (λ), an orbital reduction factor (κ) related to percent electron delocalization from metal to ligand, and an axial splitting parameter (Δ), which represents the energy between states that arise from tetragonal distortions of octahedral geometry.[36] In this case, when $S = {}^3/_2$ and $g = 2.00$, a good fit ($R = 0.0004862$) is obtained for $\Delta = 850$ cm^{-1}, $\lambda = -127$ cm^{-1}, $\kappa = 0.93$, and TIP $= 411 \times 10^{-6}$ emu mol^{-1} (Figure 2). For comparison, the free Co^{II} ion has $\Delta = 0$ cm^{-1}, $\lambda = -170$ cm^{-1}, and $\kappa = 1.00$. Compared to octahedral complexes with similar ligand field environments in the literature, **1** has a similar κ value, but a larger Δ value and a more positive λ value. See Table S3 in the SI for a full listing of the literature values.

Interestingly, a large and positive Δ value is usually associated with tetragonally compressed octahedral Co^{II} complexes,[37] in which case the $^4A_{2g}$ ground term is well isolated from the ^4E_g excited state and zero-field splitting can be extracted from a straightforward spin Hamiltonian.[38] Note that a comparable, albeit poorer, MagSaki fit to the susceptibility data uses a negative Δ value of about -550 cm^{-1}; in that case zero-field splitting parameters are not easily extracted from a spin-only Hamiltonian.[39] Assuming $\Delta \gg 0$, fits to the susceptibility and magnetization data using $S = {}^3/_2$ models in the julX[40] and ANISOFIT[27] programs, respectively, give commensurate magnetic parameters (see Supporting Information) with large $|D|$ and $|E|$ values, consistent with sizable axial and rhombic anisotropy. In depth magnetic understandings of **1** and **2** are being pursued by dynamic magnetic studies.

Temperature-dependent magnetic susceptibility data for powdered **2** encased in eicosane are presented in Figure 3. Such sample treatment is required to avoid torquing of crystallites, even in fields as small as 0.1 T. The room temperature $\chi_M T$ value of 3.72 emu K mol^{-1} is larger than the spin-only value (3.00 emu K mol^{-1}) predicted for an $S = 2$ complex with $g = 2.00$. Like Co^{II}, spin-orbit coupling is common for Fe^{II}, so larger $\chi_M T$ values are frequently encountered. The $\chi_M T$ value decreases gradually from 3.72 to 3.46 emu K mol^{-1} at 55 K, followed by a downturn to 1.92 emu K mol^{-1} at 5 K, likely as a result of zero-field splitting.

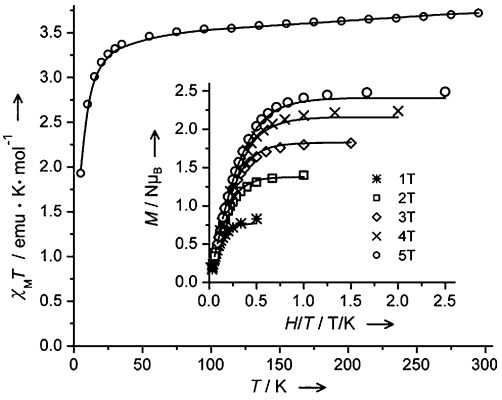

Figure 3. Temperature dependence of $\chi_M T$ for **2**, measured at 0.1 T. The best fit to the data is shown as a solid line. Inset: Field dependence of the magnetization for **2**, measured at five fields. Best fits of the data are shown as solid lines. See text for details of the fitting procedures.

Magnetization data were also obtained for **2** at dc fields between 0.1 and 5 T (Figure 3, inset). The high-field magnetization saturates at 2.5 N μ_B, lower than the 4 N μ_B expected for an isotropic system, but consistent with axial anisotropy. Using ANISOFIT,[27] fits with final parameters $g = 2.15$, $D = -11.93$ and $E = 1.47$ ($f = 0.023$) are obtained.

Fitting the susceptibility data with julX[40] where the E/D ratio was constrained to the ANISOFIT-determined value (Figure 3) supports an $S = 2$ spin state: the parameters $g = 2.15$, $D = 12.01$ cm^{-1}, $E/D = 0.12$ (fixed) and TIP $= 875 \times 10^{-6}$ emu mol^{-1} provide a good fit ($f = 0.018$). Although octahedral Fe^{II} complexes typically exhibit TIP $\approx 200 \times 10^{-6}$ emu mol^{-1}, we have previously observed large TIP for a highly anisotropic FePt complex.[41] Freely refined julX parameters, including E/D, also agree well with the results from the magnetization study (see Supporting Information for more details). Admixture of large D with spin-orbit coupling from low-lying excited states may be responsible for the smaller-than-expected saturation values observed in the magnetization data.[42] In general, however, the magnetic data for **2** are consistent with an anisotropic $S = 2$ state.

The EPR spectrum of **1** (Figure S7) gives g values of 6.84, 2.78, and 1.67. Due to the unique nature of this compound, no

other similar spectra are available for comparison, but the highly anisotropic spectrum is consistent with the structural data.

Cyclic voltammetry of **1** in CH_2Cl_2 (Figure S8) shows a quasi-reversible $Co^{III/II}$ couple with the oxidation wave at 0.125 V (vs $[Cp_2Fe]^+/[Cp_2Fe]$) and the return wave at −0.506 V. The reduction of **1** in THF (Figure S9) takes place at a largely negative potential of −2.853 V with a smaller pre-reduction feature at −2.549 V. The return wave shows a small feature at −2.190 V and a larger feature at −0.938 V. Cyclic voltammetry of **2** in MeCN (Figure S10) shows an oxidation feature at −0.348 V (vs $[Cp_2Fe]^+/[Cp_2Fe]$) and a reduction feature at −1.317 V. The low oxidation potentials indicate that a weak oxidant could effect formation of M^{III} complexes, and such studies are underway. Similar CV experiments were performed with **3** as a control (Figures S11, S12) and no features were present in the same potential range, indicating that all features are metal based.

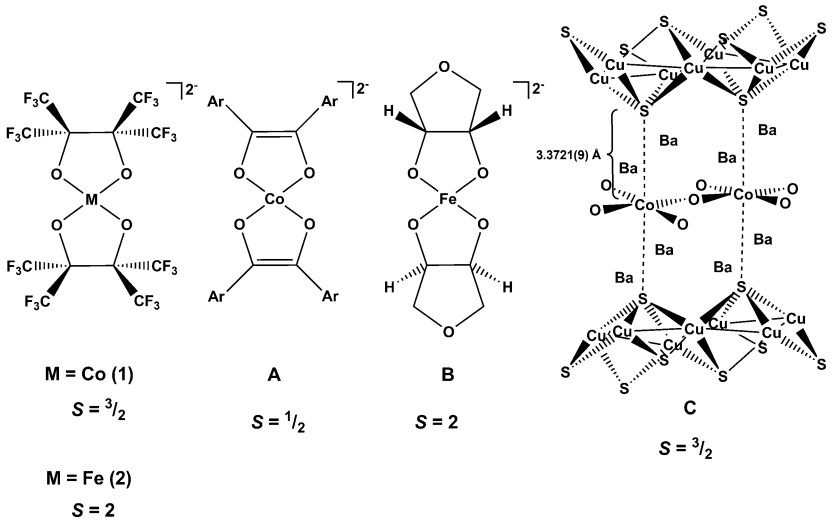

Scheme 1. Ligand and spin-state comparison of $\{MO_4\}$ compounds.

The exceedingly rare combination of square-planar geometry and high-spin state in **1** and **2** prompted careful consideration of the factors responsible. Forty years ago, Lever predicted[43] that strong π-donation would be important in stabilizing high-spin, square-planar systems, including the still unknown ^3E_g ground state for Ni^{II}. To further understand what makes this combination possible in our systems, we investigated other square-planar $\{MO_4\}$ complexes.

Scheme 1 shows five $\{MO_4\}$ complexes with square-planar geometry, two from this report and three from the literature. The first literature compound, enediolate **A**,[44] is low spin, showing that an approximately D_{4h} CoO_4 environment with π-donors does not guarantee a high-spin configuration. The average Co–O distance in **A**, 1.8713(9) Å, is shorter than that of **1**, owing to lack of fluorination on the enediolate ligand. The average O-Co-O angle bridged by the enediolate ligand is 86.59(4)°, with the Na^+ bridged O-Co-O angle of 93.41(4)°. A molecular high-spin, square-planar $\{FeO_4\}$ compound, **B**,[15,45] as well as an extended lattice, solid-state example[46] of high-spin, square-planar $\{CoO_4\}$, in the layered oxychalcogenide $Ba_2CoO_2Cu_2S_2$ phase **C**, were recently communicated. The iron diolate **B** has an average Fe–O distance of 1.99(19) Å, a τ_4 value of 0, a chelate bridged O-Fe-O angle of 84.41(5)°, and the unbridged angle of 95.59(5)°. The extended lattice, solid state example, $Ba_2CoO_2Cu_2S_2$ (**C**), has a Co^{II} center with an average Co–O distance of 2.03560(10) Å, an average O_{cis}-Co-O_{cis} angle of exactly 90.0° and a $\tau_4 = 0$. Together these five examples demonstrate the ligand features that do and do not engender square-planar, high-spin configurations.

Compound **B** is a rare molecular example of high-spin, square-planar $\{MO_4\}$ coordination without a macrocycle. A Jahn–Teller effect was proposed to play a role in favoring approximately D_{4h} over approximately T_d coordination in the $\{FeO_4\}$-containing **B**, by splitting the formerly singly occupied *e* set of orbitals, lowering the energy of the d_{z^2} orbital, and some steric repulsion of the d_{z^2} β-spin electron with the oxygen lone pairs. This proposed Jahn–Teller effect cannot be a general feature of $[Fe(OR)_4]^{2-}$ compounds, however, because the $[Fe(OC_6F_5)_4]^{2-}$ anion, $\tau_4 = 0.76$,[18] exhibits no more distortion from T_d geometry than the non-Jahn–Teller d^7 $[Co(OC_6F_5)_4]^{2-}$, $\tau_4 = 0.79$,[19] or the d^8 $[Ni(OC_6F_5)_4]^{2-}$, $\tau_4 = 0.74$.[20] Notably, the $[Cu(OC_6F_5)_4]^{2-}$ ion[19] exhibits rigorously planar $\{CuO_4\}$ coordination, demonstrating that no steric factors prevent approximately D_{4h} coordination in the $[M(OC_6F_5)_4]^{2-}$ family.

Scheme 2 shows the changes in d-orbital splitting pattern upon reduction in symmetry from O_h to D_{4h} and D_{2h}. Removal of ligands along the *z*-axis lowers the energy of the d_{z^2}, d_{xz}, and d_{yz} orbitals. Introduction of a chelate ring along the *x*-axis will raise the d_{xz} orbital energy above that of d_{yz}. Computational studies (all-electron, TZ2P GGA-BP density functional

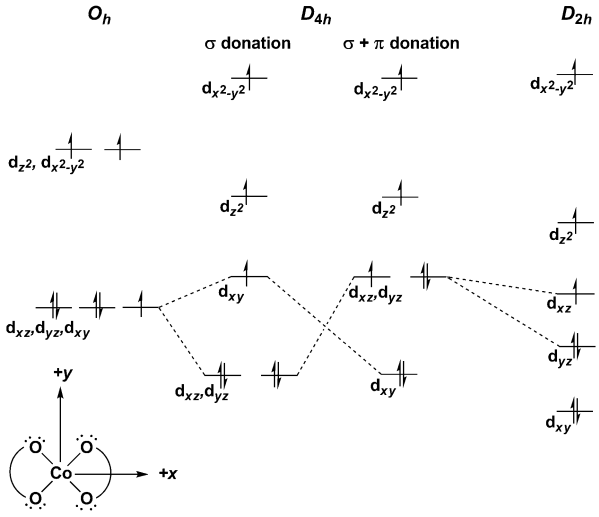

Scheme 2. Changes in the high-spin, d^7 d-orbital splitting pattern upon symmetry reduction from O_h to D_{2h}.

theory[47]) were undertaken to understand why both an oxide lattice in **C** and diolate ligand in **B** could support the high-spin, square-planar configuration, but not the diolate in **A**.

The electronic structure of **1**, and the perhydro analogue **1**-H, (distances and angles in Table S4) revealed a d-orbital splitting pattern in C_{2h} symmetry forced by the non-planar nature of the ligand, similar to the D_{2h} pattern predicted in Scheme 2 and shown in Figure S13. The major difference between qualitative Scheme 2 and the computational result is that the d_{yz} orbital is shown to be above the d_{z^2}, as a result of much greater oxygen π-donation along the *y*-axis than the *x*-axis. The $[Co(pinacolate)_2]^{2-}$ ion is unknown, probably because of the more Lewis basic character of the oxygen atoms (compared to those in $ddfp^{2-}$) which would therefore favor an octahedral, bridging oligomeric structure as observed in $\{Co(acac)_2\}$.[9]

The energies of **1** and **2** were then studied as a function of the dihedral angle between the two $\{MO_2\}$ planes of each chelating ligand, as defined in Scheme 3, and the results are shown in Figure 4. The lowest energy conformation for the

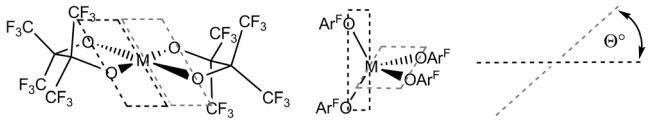

Scheme 3. $\{MO_2\}$ Planes used to calculate dihedral angles Θ in $[M(ddfp)_2]^{2-}$ and $[M(OC_6F_5)_4]^{2-}$.

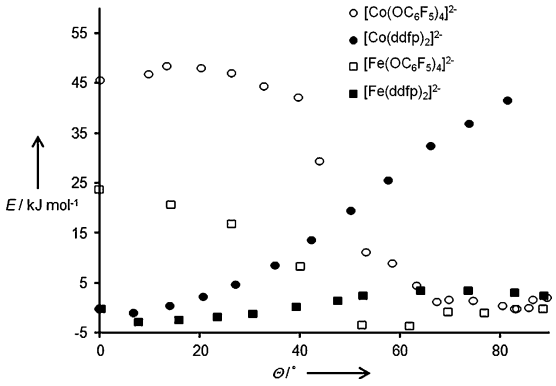

Figure 4. Relative energy of high-spin $[M(OR)_4]^{2-}$ species versus dihedral angle Θ°: $[Co(OC_6F_5)_4]^{2-}$ (○), $[Fe(OC_6F_5)_4]^{2-}$ (□), $[Co(ddfp)_2]^{2-}$ (●) and $[Fe(ddfp)_2]^{2-}$ (■).

$[M(ddfp)_2]^{2-}$ compounds is clearly much closer to square-planar than tetrahedral. In contrast, a similar linear transit study of the known $[M(OC_6F_5)_4]^{2-}$ ions, shows that these compounds with only monodentate ligands and dihedral angles of 76.9° (Co)[19] and 80.5° (Fe),[18] are much more stable in a tetrahedral geometry than square-planar, although the square-planar $[Cu(OC_6F_5)_4]^{2-}$ is also known.[19] In the absence of the chelate rings, four electronically similar donor groups give quite a distinct result.

The low-spin nature of compound **A** demonstrates that CoO_4, bis-chelate coordination can engender both high-spin and low-spin configurations, depending on the ligand structural details. Compounds **1**, **2**, and **B** have alkane diolate electronic structures, whereas **A** contains an enediolate. The latter ligand therefore has empty C=C π* orbitals which are energetically intermediate among the d-orbitals and favor a low-spin configuration with an empty $d_{x^2-y^2}$ orbital.[44] The alkane diolates have very high energy C–C or C–O σ* orbitals which are far above the d-manifold and thus high-spin configurations are observed in **1**, **2**, and **B**.

In the layered oxychalcogenide phase **C**, the high-spin state and large unquenched orbital moment were attributed to decreasing separation of the three lowest energy d-orbitals with increasing tetragonal distortion.[46] In that compound, the singly occupied $d_{x^2-y^2}$ and d_{xy} orbitals are higher in energy than the other three, which share one unpaired electron among them. The calculated ligand field in that system is therefore distinct from that in **1**, due to the greater degree of π-donation per Co in **1**, but the resulting high-spin configurations are the same.

In conclusion, we have reported the first example of a high-spin, square-planar $\{Co^{II}O_4\}$ in a molecular system and the second of a high-spin, square-planar $\{Fe^{II}O_4\}$ coordination. The combination of high-spin electron configuration and square-planar geometry is made possible by ligand constraints that generate five non-degenerate d-orbitals with ligand-based π-donation, a relatively weak ligand-field splitting, and no intervening ligand-based π-acceptor molecular orbitals. Therefore this phenomenon is enforced by the ligands, and not any particular electron count at the metal center.

Received: August 27, 2011
Revised: November 8, 2011
Published online: December 9, 2011

Keywords: cobalt · electronic structure · high-spin complexes · iron · square-planar complexes

[1] B. N. Figgis, M. A. Hitchman, *Ligand Field Theory and Its Applications*, Wiley-VCH, New York, **2000**, p. 354.
[2] J. Cirera, P. Alemany, S. Alvarez, *Chem. Eur. J.* **2004**, *10*, 190–207.
[3] J. Cirera, E. Ruiz, S. Alvarez, *Inorg. Chem.* **2008**, *47*, 2871–2889.
[4] A. R. Hermes, R. J. Morris, G. S. Girolami, *Organometallics* **1988**, *7*, 2372–2379; M. D. Fryzuk, D. B. Leznoff, S. J. Rettig, J. V. G. Young, *J. Chem. Soc. Dalton Trans.* **1999**, 147–154; J. J. H. Edema, S. Gambarotta, A. Meetsma, B. F. Van, A. L. Spek, W. J. J. Smeets, *Inorg. Chem.* **1990**, *29*, 2147–2153; R. T. Henriques, E. Herdtweck, F. E. Kuehn, A. D. Lopes, J. Mink, C. C. Romao, *J. Chem. Soc. Dalton Trans.* **1998**, 1293–1298; L. F. Larkworthy, G. A. Leonard, D. C. Povey, S. S. Tandon, B. J. Tucker, G. W. Smith, *J. Chem. Soc. Dalton Trans.* **1994**, 1425–1428; J. J. H. Edema, S. Gambarotta, B. F. Van, W. J. J. Smeets, A. L. Spek, M. Y. Chiang, *J. Organomet. Chem.* **1990**, *389*, 47–59; S. Hao, S. Gambarotta, C. Bensimon, *J. Am. Chem. Soc.* **1992**, *114*, 3556–3557; P. J. Alonso, J. Fornies, M. A. Garcia-Monforte, A. Martin, B. Menjon, C. Rillo, *Chem. Eur. J.* **2002**, *8*, 4056–4065; J. Forniés, A. Martin, L. F. Martin, B. Menjon, H. Zhen, A. Bell, L. F. Rhodes, *Organometallics* **2005**, *24*, 3266–3271.
[5] W. Bronger, S. Hasenberg, G. Auffermann, *J. Alloys Compd.* **1997**, *257*, 75–81.

[6] B. M. Reinhard, A. Lagutschenkov, J. Lemaire, P. Maitre, P. Boissel, G. Niedner-Schatteburg, *J. Phys. Chem. A* **2004**, *108*, 3350 – 3355.

[7] T. Frömmel, W. Peters, H. Wunderlich, W. Kuchen, *Angew. Chem.* **1992**, *104*, 632 – 633; *Angew. Chem. Int. Ed. Engl.Angew. Chem. Int. Ed.* **1992**, *31*, 612 – 613 (See also J. F. King, M. S. Gill, *Angew. Chem.* **1995**, *107*, 1778 – 1780; *Angew. Chem. Int. Ed. Engl.* **1995**, *34*, 1612 – 1613; T. Frömmel, W. Peters, H. Wunderlich, W. Kuchen, *Angew. Chem.* **1993**, *105*, 926 – 928; *Angew. Chem. Int. Ed. Engl.* **1993**, *32*, 907 – 909 (See also D. A. Annis, O. Helluin, E. N. Jacobsen, *Angew. Chem.* **1998**, *110*, 2010 – 2012; *Angew. Chem. Int. Ed.* **1998**, *37*, 1907 – 1909; A. Brück, U. Englert, W. Kuchen, W. Peters, *Chem. Ber.* **1996**, *129*, 551 – 555.

[8] F. A. Cotton, R. C. Elder, *J. Am. Chem. Soc.* **1964**, *86*, 2294 – 2295.

[9] F. A. Cotton, R. H. Holm, *J. Am. Chem. Soc.* **1960**, *82*, 2979 – 2983.

[10] F. H. Allen, *Acta Crystallogr. Sect. B* **2002**, *58*, 380 – 388.

[11] The τ_4 value is a geometry index useful for quantifying the geometry of four-coordinate complexes, with square-planar complexes having $\tau_4 = 0$ and tetrahedral having $\tau_4 = 1$.; L. Yang, D. R. Powell, R. P. Houser, *Dalton Trans.* **2007**, 955 – 964.

[12] J. Jubb, D. Jacoby, C. Floriani, A. Chiesi-Villa, C. Rizzoli, *Inorg. Chem.* **1992**, *31*, 1306 – 1308.

[13] C. A. Nijhuis, E. Jellema, T. J. J. Sciarone, A. Meetsma, P. H. M. Budzclaar, B. Hessen, *Eur. J. Inorg. Chem.* **2005**, 2089 – 2099; S. De Angelis, E. Solari, C. Floriani, A. Chiesi-Villa, C. Rizzoli, *J. Am. Chem. Soc.* **1994**, *116*, 5702 – 5713.

[14] V. Esposito, E. Solari, C. Floriani, N. Re, C. Rizzoli, A. Chiesi-Villa, *Inorg. Chem.* **2000**, *39*, 2604 – 2613.

[15] X. Wurzenberger, H. Piotrowski, P. Klüfers, *Angew. Chem.* **2011**, *123*, 5078 – 5082; *Angew. Chem. Int. Ed.* **2011**, *50*, 4974 – 4978.

[16] B.-S. Kang, Z.-N. Chen, Y.-X. Tong, H.-Q. Liu, H.-R. Gao, B.-M. Wu, T. C. W. Mak, *Polyhedron* **1997**, *16*, 1731 – 1737.

[17] M. Bonamico, V. Fares, A. Flamini, N. Poli, *J. Chem. Soc. Dalton Trans.* **1992**, 3273 – 3280.

[18] S. A. Cantalupo, H. E. Ferreira, E. Bataineh, A. J. King, M. V. Petersen, T. Wojtasiewicz, A. G. DiPasquale, A. L. Rheingold, L. H. Doerrer, *Inorg. Chem.* **2011**, *50*, 6584 – 6596.

[19] M. C. Buzzeo, A. H. Iqbal, C. M. Long, D. Millar, S. Patel, M. A. Pellow, S. A. Saddoughi, A. L. Smenton, J. F. C. Turner, J. D. Wadhawan, R. G. Compton, J. A. Golen, A. L. Rheingold, L. H. Doerrer, *Inorg. Chem.* **2004**, *43*, 7709 – 7725.

[20] B. N. Zheng, M. O. Miranda, A. G. DiPasquale, J. A. Golen, A. L. Rheingold, L. H. Doerrer, *Inorg. Chem.* **2009**, *48*, 4274 – 4276.

[21] M. V. Childress, D. Millar, T. M. Alam, K. A. Kreisel, G. P. A. Yap, L. N. Zakharov, J. A. Golen, A. L. Rheingold, L. H. Doerrer, *Inorg. Chem.* **2006**, *45*, 3864 – 3877.

[22] S. A. Cantalupo, J. S. Lum, M. C. Buzzeo, C. Moore, A. G. DiPasquale, A. L. Rheingold, L. H. Doerrer, *Dalton Trans.* **2010**, *39*, 374 – 383.

[23] We abbreviate the alcoholate with $(ddfp)^{2-}$ for dodecafluoropinacolate, because PFP/pfp has been used ambiguously with both perfluorophenyl (C_6F_5) and perfluoropinacolate. C. J. Willis, *Coord. Chem. Rev.* **1988**, *88*, 133 – 202.

[24] M. Allan, C. J. Willis, *J. Am. Chem. Soc.* **1968**, *90*, 5343 – 5344.

[25] C. J. Willis, *J. Chem. Soc. Chem. Commun.* **1974**, 117 – 118.

[26] H. Sakiyama, *MagSaki*,Yamagata University Department of Material and Biological Chemistry; Yamagata, **2007**, http://www-kschem0.kj.yamagata-u.ac.jp/~sakiyama/mstop.html.

[27] M. P. Shores, J. J. Sokol, J. R. Long, *J. Am. Chem. Soc.* **2002**, *124*, 2279 – 2292.

[28] F. A. Cotton, G. Wilkinson, *Advanced Inorganic Chemistry*, 4th ed., Wiley-Interscience, New York, **1980**, p. 1396.

[29] A. B. P. Lever, *Inorganic Electronic Spectroscopy*, Elsevier, New York, **1984**, p. 864.

[30] D. F. Evans, *J. Chem. Soc.* **1959**, 2003 – 2005; S. K. Sur, *J. Magn. Reson.* **1989**, *82*, 169 – 173.

[31] G. L. Miessler, D. A. Tarr, *Inorganic Chemistry*, Prentice Hall, Upper Saddle River, NJ, **1998**, p. 642.

[32] D. Christodoulou, M. G. Kanatzidis, D. Coucouvanis, *Inorg. Chem.* **1990**, *29*, 191 – 201.

[33] S. A. Carabineiro, L. C. Silva, P. T. Gomes, L. C. J. Pereira, L. F. Veiros, S. I. Pascu, M. T. Duarte, S. Namorado, R. T. Henriques, *Inorg. Chem.* **2007**, *46*, 6880 – 6890.

[34] I. Krivokapic, M. Zerara, M. L. Daku, A. Vargas, C. Enachescu, C. Ambrus, P. Tregenna-Piggott, N. Amstutz, E. Krausz, A. Hauser, *Coord. Chem. Rev.* **2007**, *251*, 364 – 378.

[35] H. Sakiyama, *Inorg. Chim. Acta* **2006**, *359*, 2097 – 2100.

[36] H. Sakiyama, *J. Comput. Chem. Jpn.* **2007**, *6*, 123 – 134.

[37] J. Titiš, R. Boča, *Inorg. Chem.* **2011**, 50, 11838—11845.

[38] R. Boča, *Coord. Chem. Rev.* **2004**, *248*, 757 – 815.

[39] R. Boča, *Struct. Bonding (Berlin)* **2006**, *117*, 1 – 264.

[40] E. Bill, *julX*,1.41; Mulheim an der Ruhr, **2008** (http://www.mpibac.mpg.de/bac/logins/bill/julX_en.php).

[41] E. W. Dahl, F. G. Baddour, W. A. Hoffert, S. R. Fiedler, M. P. Shores, G. T. Yee, J.-P. Djukic, J. W. Bacon, A. L. Rheingold, L. H. Doerrer, *Chem. Sci.* **2012**, DOI: 10.1039/C1SC00608H.

[42] S. K. Langley, R. A. Stott, N. F. Chilton, B. Moubaraki, K. S. Murray, *Chem. Commun.* **2011**, *47*, 6281 – 6283; G. Juhász, R. Matsuda, S. Kanegawa, K. Inoue, O. Sato, K. Yoshizawa, *J. Am. Chem. Soc.* **2009**, *131*, 4560 – 4561.

[43] J. C. Donini, B. R. Hollebone, A. B. P. Lever, *J. Am. Chem. Soc.* **1971**, *93*, 6455 – 6462.

[44] G. H. Spikes, C. Milsmann, E. Bill, T. Weyhermuller, K. Wieghardt, *Inorg. Chem.* **2008**, *47*, 11745 – 11754.

[45] P. L. Holland, *Nat. Chem.* **2011**, *3*, 507 – 508.

[46] C. F. Smura, D. R. Parker, M. Zbiri, M. R. Johnson, Z. n. A. Gál, S. J. Clarke, *J. Am. Chem. Soc.* **2011**, *133*, 2691 – 2705.

[47] G. te Velde, F. M. Bickelhaupt, E. J. Baerends, C. Fonseca Guerra, S. J. A. van Gisbergen, J. G. Snijders, T. Ziegler, *J. Comput. Chem.* **2001**, *22*, 931 – 967.

[48] CCDC 841985 (**1**), 841986 (**2**), and 841987 (**3**) contain the supplementary crystallographic data for this paper. These data can be obtained free of charge from The Cambridge Crystallographic Data Centre via www.ccdc.cam.ac.uk/data_request/cif.

